Combust. Sci. and Tech., 1986, Vol. 48, pp. 241–255
0010-2202/86/4806-0241 $25.00/0

Chemical and Optical Probing of Premixed Methane/Oxygen Flames

EVERETT R. RAMER and JOSEPH F. MERKLIN *Department of Nuclear Engineering, Kansas State University, Manhattan, KS 66506*

CHRISTOPHER M. SORENSEN and THOMAS W. TAYLOR *Department of Physics, Kansas State University, Manhattan, KS 66506*

(Received July 8, 1985; in final form October 28, 1985)

Abstract—We have measured the concentration profiles of the major products in fuel-rich premixed CH_4/O_2 flames. Optical measurements were performed to measure soot number densities, volume fraction and particle size distributions. We have shown that the increase in the soot volume fraction is due to surface growth and that acetylene is the source of the carbon involved in this process. We have also been able to determine the importance of coagulation versus surface growth in the increase of soot particle radius with time in these flames.

INTRODUCTION

Formation of soot in a flame has certainly been the object of intense study by many in the field of combustion research. In their book on flames, Gaydon and Wolfhard (1979) summarize much of the work that has been done with regard to answering this question. From their arguments, and those published more recently by other workers (D'Alessio *et al.*, 1975; Harris and Weiner, 1983a, 1983b, 1984), the appearance of soot in premixed flames can be separated into two distinct, but not completely independent events: soot particle inception and soot particle surface growth. These events are distinct in that they dominate in different regions of the premixed flame and may be the result of differing chemical processes. They are not independent, however, since the extent of surface growth in premixed flames is controlled by the inception event.

In their study of premixed ethylene flames, Harris and Weiner found that the soot mass growth rate increased rapidly as the fuel/oxidizer ratio increased. They noted, however, that the total soot surface area was also a strong function of the fuel/oxidizer ratio and that consequently the specific soot mass growth rate (*i.e.*, growth rate per unit surface area) was nearly independent of the fuel/oxidizer ratio. This leads to the important conclusion that as the fuel/oxidizer ratio is increased a premixed flame gets sootier largely because its soot surface area increases. However, since the surface area present at the onset of surface growth depends on the amount of soot produced by inception, the outcome of inception clearly influences the mass of soot produced by the premixed flame. Thus, as a premixed flame's fuel/oxidizer ratio increases, it gets sootier because particle inception increases the total surface area available for growth.

The control held over soot mass by inception is, however, only partial. In addition to its dependence on surface area, Harris and Weiner found that the rate of soot mass increase in a premixed flame also depended, to first order, on the concentration of acetylene in the burned gas region of the premixed flame. This means that as the

fuel/oxidizer ratio increases, the premixed flame becomes sootier because of the concerted effect of increases in both inception and burned-gas acetylene concentration.

In this paper we report measurements of the chemical and optical properties of premixed methane–oxygen flames. Our chemical probing yielded the major burned-gas phase mole fractions, including water. The water mole fraction was determined in a new way by enforcing an oxygen balance on the product species. Optical measurements were performed to study soot growth characteristics. Scattering/extinction measurements were used to determine soot number densities and volume fractions. In addition, photon correlation spectroscopy allowed us to determine the effective first two moments of the soot particle size distribution which we take to be log-normal.

Our results support the conclusions of Harris and Weiner that the specific soot mass growth rate is only weakly dependent on the fuel/oxidizer ratio and that this rate depends on the acetylene concentration to first order. In fact, our surface growth rate constant is essentially the same as theirs, suggesting that this quantity may be independent of the fuel used and universal to all premixed flames. We also show the effects of surface growth on the soot particle size distribution, and compare quantitatively the rates of soot particle size increase from coagulation and surface growth.

EXPERIMENTAL PROCEDURE

We burned premixed flames of methane and oxygen at atmospheric pressure on a 6 cm diameter flat-flame burner (McKenna Products). Surrounding the water-cooled frit was a 0.5 cm wide annular nitrogen sheath. A 15 cm diameter steel stagnation plate was mounted 2.9 cm above the burner.

The fuel/oxidizer ratios we studied were 1.09, 1.22 and 1.41. All gas flowrates were controlled using critical orifices, which we calibrated using a dry-test flowmeter. A linear velocity of 6 cm/s at 25°C was maintained for the unburned fuel–oxygen mixture. The nitrogen sheath flow velocity was 18 cm/s. Cooling water flowed through the frit at a rate of about 1 l/min and suffered no appreciable increase in temperature.

Samples of burned gas were removed from the flame using an uncooled quartz probe. We constructed this probe by drawing out the end of a 0.4 cm (i.d.) quartz-to-Kovar seal. As a consequence, it was relatively easy to establish a dependable joint between the probe and the metal sampling system. The probe was mounted vertically (*i.e.*, perpendicular to the burner surface) and was lowered down into the flame through a 1 cm diameter hole cut in the stagnation plate. Height of the probe was measured using a cathetometer. The probe orifice diameter was 0.05 cm. The probe was deliberately made very blunt (apex angle of 40°) to cause rapid expansion of the sample and to reduce plugging of the orifice by soot.

Pressure inside the burned gas sampling system was maintained at 100–300 torr in order to insure critical flow through the probe orifice. Gas samples were analyzed using a gas chromatograph (Carle model S311). We used a gas sampling box (Chedaille and Braud, 1972) to overcome the problem of introducing samples collected at a low pressure into the sampling valve of the chromatograph, which was under atmospheric pressure. This box was made by enclosing a Halar gas sampling bag in a gas-tight container. The bag was attached to the sampling line and was filled by pumping on the container. After the bag was removed from the system, the sample pressure was increased by pressurizing the container with helium.

A thermal conductivity detector was used to measure burned gas mole fractions of H_2, O_2, CO, CO_2, C_1's and C_2's. Mole fractions of C_3's and C_4's were obtained from a flame ionization detector. Both detectors were calibrated using commercial standards (Scott can mixes 216 and 234), thus our mole fractions were absolute. Since water condensed out of the sample, the mole fractions given by the chromatograph were considered to be on a dry basis. From these mole fractions, the actual flame mole fractions were calculated as follows. We first established a carbon balance between the analyzed flame sample and the unburned fuel–oxygen mixture whose composition was known. This balance assumed that a negligible amount of carbon was transformed into undetectable species: soot, PAHs, etc. The information obtained from this balance was then used to predict the oxygen content of the flame sample. All undetected oxygen was assumed to have been converted to water. Once the mole fraction of water in the flame was known, the dry-basis mole fractions obtained from the chromatograph could be modified to their actual flame values. Comparison of the elemental contents of the unburned gas and the flame showed that we accounted for better than 95 percent of the incoming atoms of each element (carbon, hydrogen and oxygen).

Photon Correlation Spectroscopy (Berne and Pecora, 1976), PCS, was performed on the flame. The optical setup consisted of an argon ion laser operating at $\lambda = 5145$ Å which was periodically checked to ensure it was in the TEM_{00} mode. The beam was collimated using a 2 m focal length lens situated 2 m from the center of the laser. Thereafter the light was focused by a double lens combination with an effective focal

TABLE I

Parameters for the three premixed methane/oxygen flames studied. Fuel/oxidizer, f/o; height above burner, Z; most probable size from PCS, r_0; geometric width, σ; number density, n; and soot volume fraction, V

f/o	Z (mm)	r_0 (mm)	σ	n (10^9 cm^{-3})	V (10^{-7})
1.09	10	—	—	—	0.9
	11	7.1	1.27	—	—
	12	9.6	1.34	14.0	1.3
	14	13.9	1.28	5.4	1.0
	16	16.6	1.28	3.3	1.0
1.22	8	17.2	1.287	8.3	2.85
	10	22.7	1.276	5.54	4.2
	12	26.6	1.270	4.28	5.15
	14	35.9	1.214	2.17	5.55
	16	45.5	1.150	1.39	6.35
1.41	6	12.7	1.285	35.6	5.06
	8	24.2	1.266	9.25	8.36
	10	32.5	1.274	5.55	12.4
	12	40.9	1.255	3.59	15.2
	14	49.5	1.250	2.37	17.4
	16	61.4	1.214	1.58	20.5

length of 2 m. This gave a focused beam waist measured to be 0.037 cm in the flame. This beam waist was large to help eliminate the effects of the beam transit term (Chowdhury *et al.*, 1984), yet not too large to hurt our coherence requirements for the photocathode or the spatial resolution of the measurement in the flame.

The scattered light was detected at small scattering angles near the forward direction. This light was collected by a lens and focused onto a 300 μ pinhole, chosen to ensure coherence on the photomultiplier 50 cm away. The output pulses from the photomultiplier were amplified and discriminated, and fed to a commercial correlator which computed the correlation function. This information was then analyzed on a laboratory computer.

A two-cumulant fit to the scattered light correlation function was performed. The first cumulant was related to the average size of the scatterers through the scattering wave vector and the free molecular diffusion coefficient. The ratio of the second cumulant to the first cumulant squared gave information regarding the second moment of the soot particle size distribution. To facilitate our analysis, we have

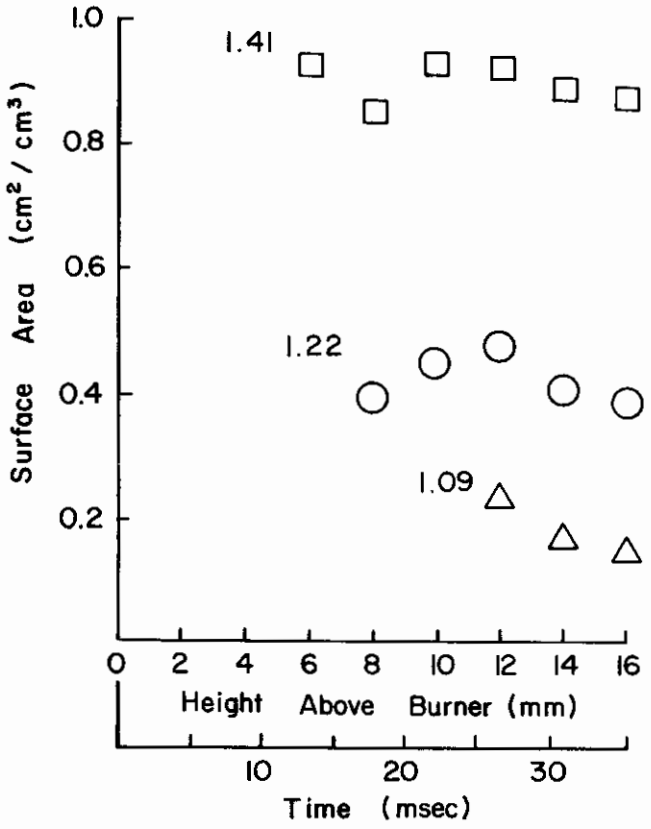

FIGURE 1 Total surface area of soot per cm^3, S, versus height above burner, Z.

assumed a zeroth-order lognormal (ZOLD) size distribution. Such a distribution is reasonable as determined by electron micrograph measurements (Lahaye *et al.*, 1974) and sufficient since we measured only the first two moments.

Static scattering/extinction measurements were also performed on the flame (D'Alessio, 1981). The scattering measurement was performed with the same photomultiplier used for the PCS measurement. Calibration of the scattering measurement was made by scattering from gaseous methane, oxygen and ethylene for which the Rayleigh cross sections are known. The extinction measurement was made using a 1P28 photomultiplier and photon counting.

The details of both light scattering measurements are given in another publication (Scrivner *et al.*, 1985). However, a brief description of the assumptions and approximations used in the analysis of the light scattering data is appropriate here. The PCS

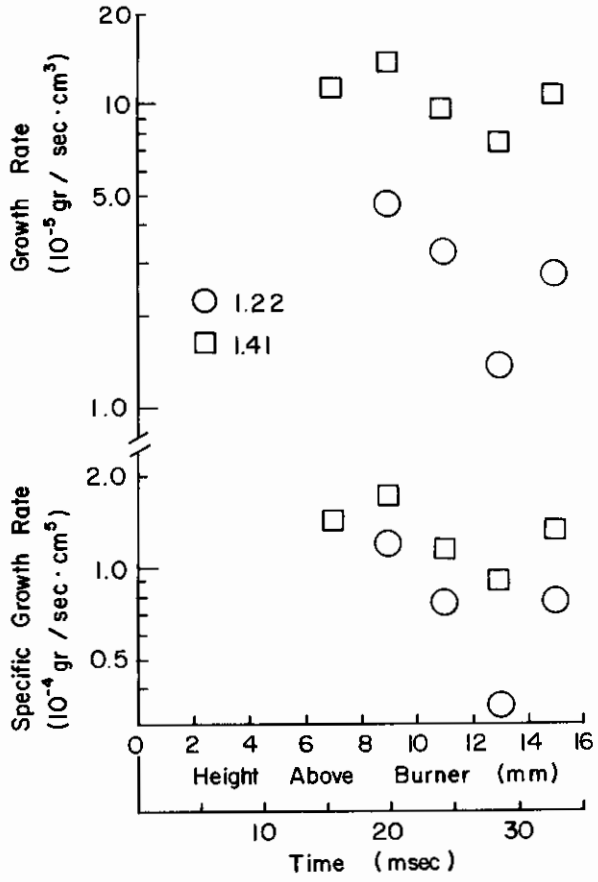

FIGURE 2 Total growth rate of soot per cm³, dm/dt, and specific growth rate of soot per cm³, $S^{-1}\, dm/dt$, versus height above burner.

technique measured the average diffusion coefficient of the soot particles in the flame. We made the reasonable assumption that the kinetic diffusion coefficient is applicable to extract the mean radius of the particles. Spurious terms due to the finite velocity of the particles and photomultiplier afterpulsing have been negated. For the scattering/extinction measurement we have assumed a particle index of refraction equal to $n=1.57-i0.56$. Both methods rely on $r \ll \lambda$ and assume the particles are spherical. Determination of the geometric width, σ, of the assumed ZOLD is complex and we refer the reader to our earlier work (Scrivner *et al.*, 1985).

An optical pyrometer was used to measure the brightness temperature of the flame at the 5145 Å wavelength of the argon laser. This pyrometer was constructed by replacing the standard red filter of a commercial instrument with a 5145 Å optical notch filter. The pyrometer was then recalibrated using a tungsten lamp. True

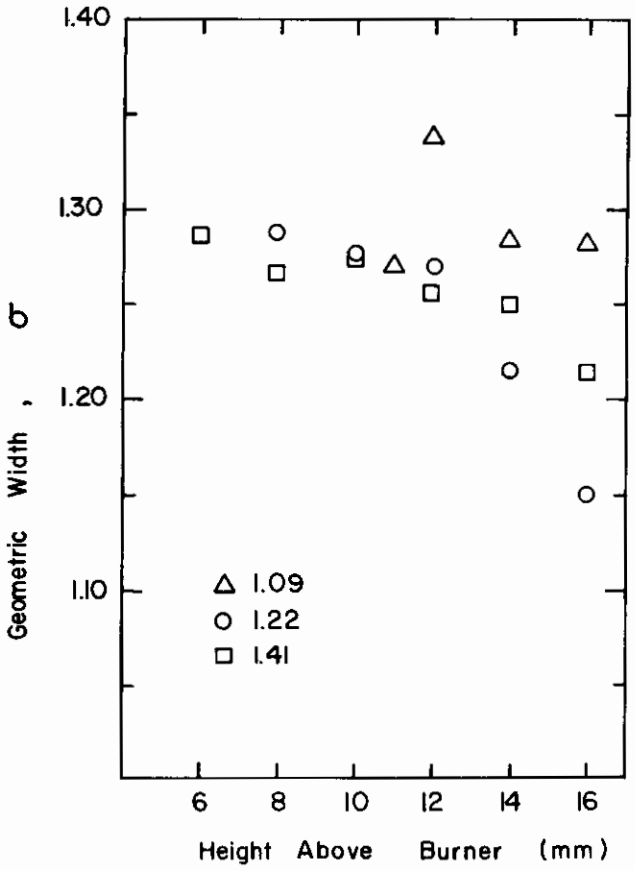

FIGURE 3 Geometric width of soot particle size distribution, σ, versus height above burner.

flame temperatures were determined via Planck's law using emissivities determined from Kirchoff's law and the absorptivity of the flame obtained from the scattering/extinction measurements.

RESULTS

Table I gives the results of our optical measurements for the three fuel/oxidizer ratios studied. The most probable size, r_0, and geometric standard deviation, σ, were determined from the PCS measurements. The number density, n, was determined

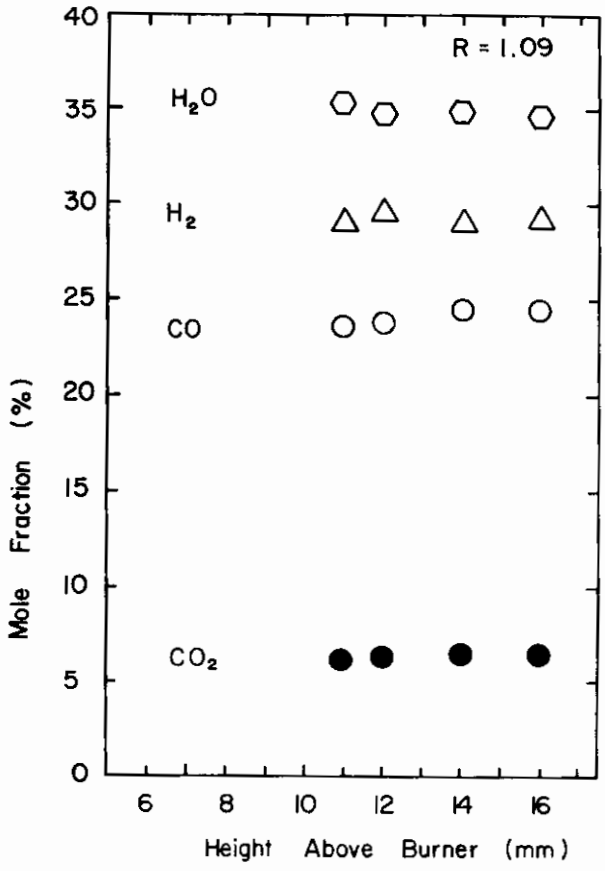

FIGURE 4 Mole fractions of the principle stable species in the $R = 1.09$ flame versus height above burner.

from the scattering intensity using r_0 and σ, and the volume fraction was determined directly from the extinction measurement.

We calculated the total surface area, S, of the soot particles using r_0, σ, and n from Table I. The results, presented in Figure 1, show the same interesting constancy of S as a function of time observed by Harris and Weiner. Similar behavior of the surface area has also been noted by Wagner (1983). To convert height above burner, Z, to time, we used an average flame temperature of 1600 K and a molar increase factor of 1.33, from our chemical analysis presented below, to convert the unburned gas velocity to flame velocity. Cross-sectional area of the flame was assumed constant.

To find the rate of soot mass increase, dm/dt, the slope of the volume fraction with respect to Z was calculated using simple linear interpolation between adjacent points in Table I. This slope was then multiplied by the flame velocity and a soot density of 1.8 g cm^{-3}. The upper part of Figure 2 shows our results for the two richest flames, the 1.09 fuel/oxidizer ratio data were not precise enough to calculate slopes.

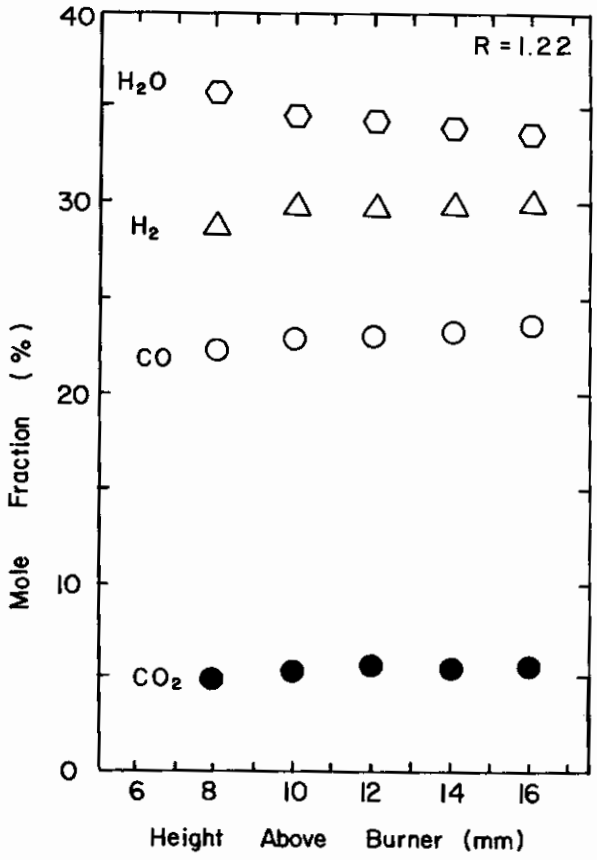

FIGURE 5 Mole fractions of the principle stable species in the $R=1.22$ flame versus height above burner.

The mass growth rates of the two flames are considerably different. However, when normalized by the surface area, from Figure 1, the specific growth rates, shown in the lower part of Figure 2, are very similar. This is the same result which led Harris and Weiner to propose that the increased soot growth rate observed as premixed flames become richer is largely a consequence of the increased surface area.

Measurement of the width parameter of the soot size distribution allows us to demonstrate another effect of surface growth. Figure 3 shows that the geometric width σ tends to decrease with increasing time above burner. This behavior can be understood in terms of surface growth. If the rate of material deposition per unit area is the same for all the soot particles in the size distribution, then all their radii will increase at the same rate regardless of size. Thus, the geometric width will

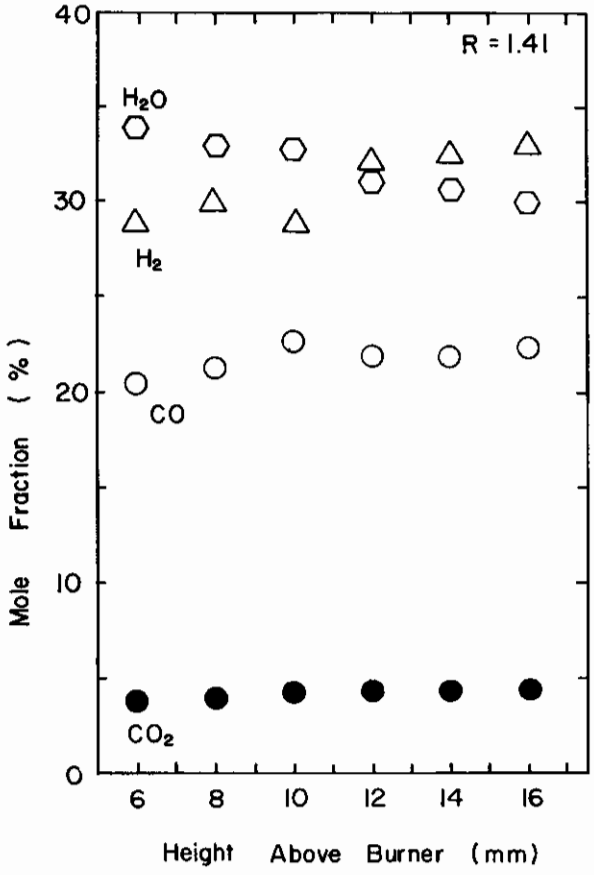

FIGURE 6 Mole fractions of the principle stable species in the $R = 1.41$ flame versus height above burner.

decrease with time as the mean size increases. This is precisely the behavior seen in Figure 3. Coagulation is also occurring, so we have not quantitatively compared the σ decrease to the surface growth rate. In fact, the absolute width increases for all time due to the coagulation process.

An overall view of the major gas phase components, except acetylene and methane, of our flames is presented in Figures 4, 5 and 6. Again, we emphasize the point that these mole fractions represent actual flame values, which have been calculated using the procedure outlined earlier. Only the region which was studied optically was chemically probed. The mole fraction profiles shift up and down as the fuel/oxidizer ratio is increased. However, they remain nearly constant for a given flame.

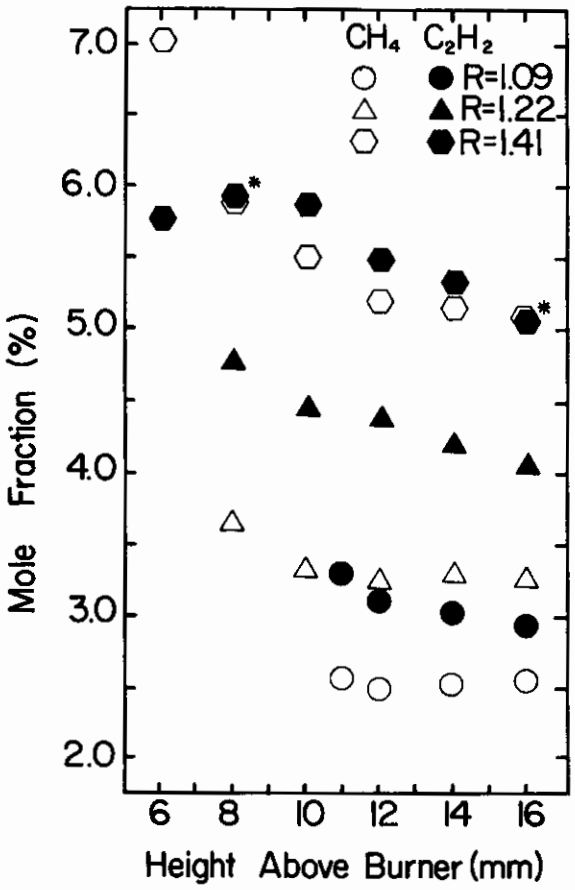

FIGURE 7 Mole fractions of acetylene and methane versus height above burner. (Asterisks indicate overlapping points.)

The mole fraction profiles of acetylene and methane are shown in Figure 7. From these data, it appears that in the region of the flame studied the mole fraction of methane is either constant or in the process of becoming so. In contrast, the acetylene profile shows no sign of leveling out.

Minor hydrocarbon species were also detected using a flame ionization detector. These results are briefly summarized as follows. The mole fraction of ethylene was observed to increase with increasing fuel/oxidizer ratio and to increase with height above burner for a given flame. Thus for the $R=1.41$ flame, the ethylene mole fraction increased from 0.25 to 0.41 percent over the region studied. C_3's and C_4's were present in amounts less than 1000 ppm and 100 ppm respectively. The mole fractions of these species were essentially constant with height above burner.

With the chemical composition and soot particle size data in hand, it would be of interest to search for the source of the carbon responsible for the soot volume fraction increase. While this source of carbon may not be the actual growth species, any growth species would have to be in rapid equilibrium with it.

Our soot volume fraction data in Table I show that in our richest flame the soot mass increases by over 2×10^{-6} g cm^{-3} from 6 mm to 16 mm above the burner. Following the argument advanced by Harris and Wiener (1983a), this sets a lower

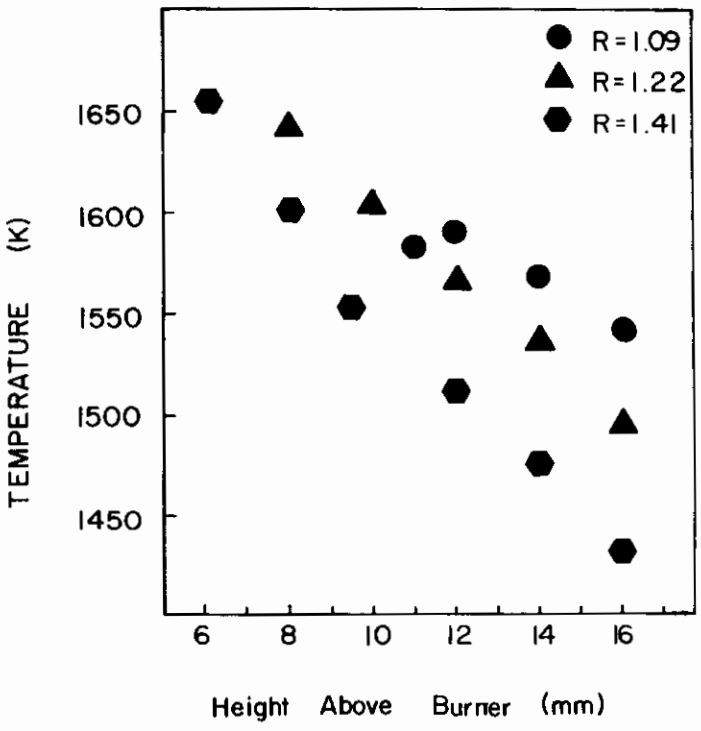

FIGURE 8 Flame temperature versus height above burner.

limit on the mole fraction of the carbon source of $0.25/W$, W being the molecular weight of the carbon source species. At 6 mm above burner in our richest flame the only hydrocarbons in excess of this limit are acetylene and methane.

Acetylene and methane loss rates can be estimated, ignoring diffusion effects, from the slopes of their mole fraction profiles in Figure 7. The required flame temperatures are given in Figure 8. A more rigorous determination of these loss rates based on diffusional fluxes (cf. Bittner and Howard, 1981; Fristrom and Westenberg, 1965) yielded results identical to those of the simple approach described above. The rates of soot mass increase can be obtained from Table I as previously outlined.

For the $R = 1.22$ flame the rate of methane loss beyond 10 mm above the burner is essentially zero. The average rate of acetylene loss is 1.6×10^{-7} g carbon cm^{-3} mm^{-1}. In this same region the soot mass increases at the rate of 6.5×10^{-8} g carbon cm^{-3} mm^{-1}. Thus, in the $R = 1.22$ flame, the carbon responsible for the soot mass increase comes either directly or indirectly from the acetylene.

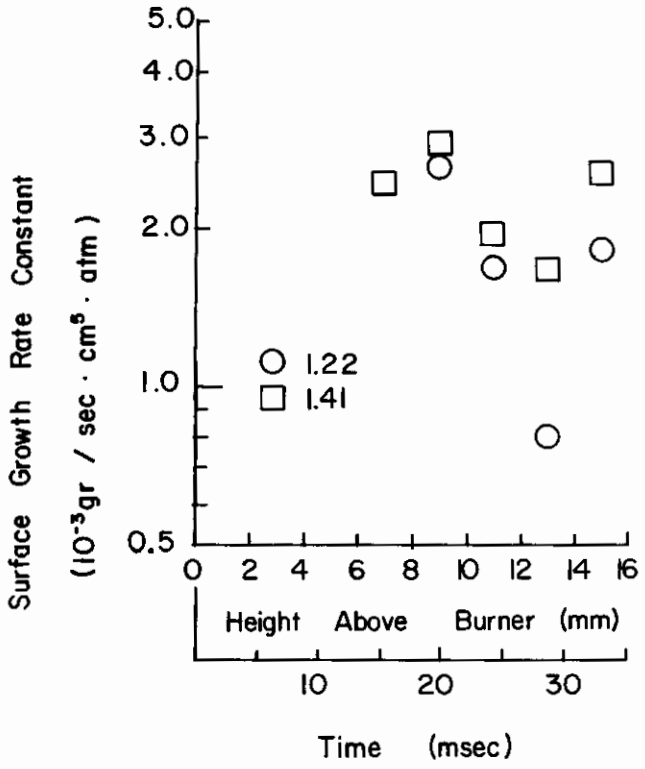

FIGURE 9 Soot surface growth rate constant, $S^{-1}\, dm/dt\, [C_2H_2]^{-1}$, versus height above burner.

The case of the $R=1.41$ flame is not so clear cut. At 10 mm above burner the loss rate of methane is 1.7×10^{-7} g carbon cm^{-3} mm^{-1}, that of acetylene is 1.0×10^{-7} g carbon cm^{-3} mm^{-1}, while the soot mass gain rate is 3.1×10^{-7} g carbon cm^{-3} mm^{-1}. However, the rate of methane disappearance decreases rapidly with height. By 14 mm above the burner the rate of soot mass gain is 2.4×10^{-7} g carbon cm^{-3} mm^{-1} and the rate of acetylene loss is 2.3×10^{-7} g carbon cm^{-3} mm^{-1}. By comparison, the rate of methane loss is only 3.5×10^{-8} g carbon cm^{-3} mm^{-1}. While contribution of methane to the soot mass increase cannot be completely ruled out in the lower portion of the region studied, only acetylene can serve as the source of carbon throughout the entire region.

Thus we are led to conclude that the soot mass increase can most consistently be related to the loss rate of acetylene. Acetylene may be the growth species. Even if it is not, the growth species must be in rapid equilibrium with acetylene.

Based on the above conclusion, we now calculate the surface growth rate constant k where

$$S^{-1}\frac{dm}{dt} = k[C_2H_2]. \tag{A}$$

We assume, as proposed by Harris and Weiner, acetylene to be the the major source of growth carbon and that the reaction is of first order. Values for the specific growth rate and acetylene mole fraction are presented in Figures 2 and 7. The values for k, given in Figure 9, are in excellent agreement with those found by Harris and Weiner in premixed ethylene and ethylene–toluene flames. This agreement suggests that the surface growth process in our respective flames is fundamentally similar and that this similarity is true for premixed flames in general. Despite the fact that our acetylene mole fractions are two to three times those measured by Harris and Weiner, our

TABLE II

Logarithmic rate of growth of the soot particle radius, $\Delta \ln r/\Delta Z$. This rate of growth should be the result of two terms, surface growth and coagulation, the sum of which is given in the last column

ΔZ (mm)	$\frac{\Delta \ln r}{\Delta Z}$ (mm^{-1})	$\frac{1}{3}\frac{\Delta \ln V}{\Delta Z}$ (mm^{-1})	$-\frac{1}{3}\frac{\Delta \ln n}{\Delta Z}$ (mm^{-1})	Sum (mm^{-1})
		1.22 Flame		
8–10	0.139	0.065	0.067	0.132
12–14	0.150	0.012	0.113	0.126
14–16	0.118	0.022	0.074	0.097
8–16	0.122	0.033	0.075	0.108
		1.41 Flame		
6–8	0.322	0.27	0.225	0.495
10–12	0.115	0.034	0.073	0.107
14–16	0.108	0.027	0.068	0.095
6–16	0.158	0.047	0.104	0.151

values of k are essentially the same. This result substantiates the claim that surface growth is a first order process.

Figure 9 shows, as was found by Harris and Weiner, that k decreases with increasing time, suggesting a decrease in soot reactivity with time. Our data show an increase in k for $Z = 1.5$ cm in both flames. We cannot at this time determine whether this is a real effect or an experimental artifact.

To demonstrate the interrelationship between coagulation and surface growth in determining the ultimate size of soot particles, we differentiate the expression

$$V = \frac{n 4\pi r^3}{3}, \tag{B}$$

to obtain

$$\frac{d \ln r}{dz} = \frac{1}{3}\frac{d \ln V}{dz} - \frac{1}{3}\frac{d \ln n}{dz}. \tag{C}$$

This result shows that the increase in r with height above the burner is due to two terms, the first being surface growth and the second due to coagulation. We have tested Eq. (C) with our data, performing simple linear differentiation of the data in Table I. The results, as given in Table II, show good consistency and help illustrate the relative importance of each growth process. Furthermore, the surface growth and the coagulation growth are in a ratio of roughly 1:2, which is necessary if the total surface area is to remain constant.

CONCLUSIONS

The major conclusion of this work is that the increase of the soot volume fraction in premixed CH_4/O_2 flames is due to surface growth. This growth is accompanied by a decrease in acetylene and the mass increase of the soot can be quantitatively related to the decrease in the acetylene mole fraction. Our estimate of the surface growth rate constant is in excellent agreement with those found by Harris and Weiner in significantly different flames, and we lend support to the first order dependence of surface growth on acetylene concentration. This further supports the speculation of Harris and Weiner that there is a single process for surface growth in premixed flames, and this process is acetylene addition. Further, we have been able to determine the importance of coagulation versus surface growth in the increase of soot particle radius with time.

ACKNOWLEDGEMENT

We thank Steve Scrivner for help with the optical measurements. This work was supported by DOE Grant DE-AC02-80ER10677.

REFERENCES

Berne, B. J., and Pecora, R. (1976). *Dynamic Light Scattering*. Wiley, New York.

Bittner, J. D., and Howard, J. B. (1981). Pre-particle chemistry in soot formation, in *Particulate Carbon*, D. C. Siegla and G. W. Smith (Eds.). Plenum, New York, p. 109.

Chedaille, J., and Braud, Y. (1972). *Industrial Flames*, Volume I, *Measurements in Flames*. Arnold, London.

Chowdhury, D. P., Sorensen, C. M., Taylor, T. W., Merklin, J. F., and Lester, T. W. (1984). Application of photon correlation spectroscopy to flowing Brownian motion systems. *Appl. Opt.* **23**, 4149.

D'Alessio, A., DiLorenzo, A., Sarofim, A. F., Beretta, F., Masi, S., and Venitozzi, C. (1975). Soot formation in methane–oxygen flames. *Fifteenth Symposium (International) on Combustion*, The Combustion Institute, p. 1427.

D'Alessio, A. (1981). Laser light scattering and fluorescence diagnostics of rich flames produced by gaseous and liquid fuels, in *Particulate Carbon*, D. C. Siegla and G. W. Smith (Eds.). Plenum, New York, p. 207.

Fristron, R. M., and Westenberg, A. A. (1965). *Flame Structure*. McGraw-Hill, New York.

Gaydon, A. G., and Wolfhard, H. G. (1979). *Flames*. Chapman and Hall, 4th edn., London.

Harris, S. J., and Weiner, A. M. (1983a). Surface growth of soot particles in premixed ethylene/air flames. *Comb. Sci. and Tech.* **31**, 155.

Harris, S. J., and Weiner, A. M. (1983b). Determination of the rate constant for soot surface growth. *Comb. Sci. and Tech.* **32**, 75.

Harris, S. J., and Weiner, A. M. (1984). Soot particle growth in premixed toluene/ethylene flames. *Comb. Sci. and Tech.* **38**, 75.

Lahaye, J. Prado, G., and Donnet, J. B. (1974). Nucleation and growth of carbon black particles during benzene decomposition. *Carbon* **12**, 27.

Scrivner, S. M., Taylor, T. W., Sorensen, C. M., and Merklin, J. F. (1985). Soot particle size distribution measurements in a premixed flame using photon correlation spectroscopy, submitted to *Appl. Opt.*

Wagner, H. Gg. (1983). Mass growth of soot, in *Soot in Combustion Systems and its Toxic Properties*, J. Lahaye and G. Prado (Eds.). Plenum, New York, p. 171.